Synthesis of monosized magnetic-optical AuFe alloy nanoparticles

Hong Ling Liu, Jun Hua Wu, Ji Hyun Min, and Young Keun Kim

Related Articles

Size dependent melting behaviors of nanocrystalline in particles embedded in amorphous matrix
J. Appl. Phys. 111, 043515 (2012)

Stretch-induced plasmonic anisotropy of self-assembled gold nanoparticle mats
Appl. Phys. Lett. 100, 073101 (2012)

Perovskite phase transformation in 0.65Pb(Mg1/3Nb2/3)O3-0.35PbTiO3 nanoparticles derived by sol-gel
J. Appl. Phys. 111, 024314 (2012)

Thermoelectric properties of Cu doped ZnSb containing Zn3P2 particles
J. Appl. Phys. 111, 023703 (2012)

Shock-induced consolidation and spallation of Cu nanopowders
J. Appl. Phys. 111, 013508 (2012)

Additional information on J. Appl. Phys.

Journal Homepage: http://jap.aip.org/

Journal Information: http://jap.aip.org/about/about_the_journal

Top downloads: http://jap.aip.org/features/most_downloaded

Information for Authors: http://jap.aip.org/authors

Synthesis of monosized magnetic-optical AuFe alloy nanoparticles

Hong Ling Liu
*Institute for Nano Science, Korea University, Seoul 136-713, Korea
and College of Chemistry and Chemical Engineering, Henan University, Kaifeng 475001,
People's Republic of China*

Jun Hua Wu[a),b)]
Research Institute of Engineering and Technology, Korea University, Seoul 136-713, Republic of Korea

Ji Hyun Min and Young Keun Kim[a),c)]
Department of Materials Science and Engineering, Korea University, Seoul 136-713, Republic of Korea

We report the preparation and characterization of multifunctional AuFe alloy nanoparticles of three compositions, $Au_{0.25}Fe_{0.75}$, $Au_{0.5}Fe_{0.5}$, and $Au_{0.75}Fe_{0.25}$, by a polyol process. It is found that the fusion of the two elements into one nanostructure entity retains the optical and magnetic properties of the individual components. The x-ray diffraction and transmission electron microscopy analyses confirm the formation of the alloy nanostructure with a narrow distribution of particle sizes and provides the detailed structural arrangements. The magnetic investigation shows the superparamagnetic or soft ferromagnetic behavior of the nanoparticles at room temperature, whereas the UV-visible measurements display the variation of the absorption bands at ~560 nm. The AuFe nanoparticles are rendered water soluble after thiolation. © *2008 American Institute of Physics*.
[DOI: 10.1063/1.2837619]

I. INTRODUCTION

Smart nanoparticles (NPs) of multiple components offer exciting opportunities in fundamental studies and highly multidisciplinary nanotechnology that has rapidly grown with tremendous applications in many areas including medicine, life science, materials science, environment, electronics, and energy. With respect to magnetic NPs, attraction arises from their reduced dimension with unique properties different from their bulk counterparts.[1–3] On the other hand, Au NPs and nanostructures are the focus in the investigation and application of the optical properties of materials.[4–6] They reveal an absorption band in the visible region as a result of surface plasmon, which is characterized by the particle size and physicochemical environment surrounding the particles.

Since fusion of the magnetic and optical elements in one single entity promises multifunctionality and potential applications, so a great deal of effort is instilled to prepare such nanoparticles containing Au and Fe.[7–12] We have investigated a variety of functional nanoparticles via an efficient, scalable, and nontoxic synthesis approach.[13,14] In this work, we report the preparation and characterization of multifunctional magnetic-optical AuFe alloy NPs via a one-pot polyol process, integrating the optical functionality of Au composition and the magnetic properties of iron.

II. EXPERIMENTAL PROCEDURE

The two precursors used are gold acetate [$Au(OOCCH_3)_3$, 99.9%] and iron (III) acetylacetonate [$Fe(acac)_3$, 99.9%]. Other chemicals include 1,2-hexadecanediol, poly(ethylene glycol)-block-poly(propylene glycol)-block-poly(ethylene glycol) (PEO-PPO-PEO), oleylamine, oleic acid, octyl ether, mercaptoethanol, hexane, and ethanol. A typical synthesis was carried out in a flask, mixing $Au(OOCCH_3)_3$ and $Fe(acac)_3$ in octyl ether with the reducing agent 1,2-hexadecanediol, surfactant, and cosurfactant such as triblock copolymer PEO-PPO-PEO or oleic acid and oleylamine under vigorous stirring. The reaction mixture was first heated and refluxed at a temperature of $80\ ^\circ C$ for 10 min and then rapidly raised to high temperature to complete the reaction. Ethanol was added to the reacted mixture to precipitate the nanoparticles after cooling down to room temperature. Three AuFe compositions in the ratios of $Au(OOCCH_3)_3$ to $Fe(acac)_3$, 3:1, 1:1, and 1:3, were prepared. The crystal structure of the synthesized AuFe NPs was acquired by x-ray diffraction (XRD) (Bruker M18XCE, $\lambda = 1.540\ 56$ A) and the nanostructures were characterized by transmission electron microscopy (TEM) (JEOL 2010F). The UV-visible spectra were performed using an Agilent 8453E spectrophotometer and the magnetic properties were obtained by a vibrating sample magnetometer (Lakeshore 7300) and a superconducting quantum interference device (SQUID).

III. RESULTS AND DISCUSSION

Three AuFe compositions, nominally $Au_{0.75}Fe_{0.25}$, $Au_{0.5}Fe_{0.5}$, and $Au_{0.25}Fe_{0.75}$, were confirmed by elemental analysis performed on the single nanoparticles of the precipitates. The crystal structure of the nanoparticles as synthesized was obtained by XRD as a function of composition, as given in Fig. 1. As labeled in the figure, the peaks at 38.14°,

---
a)Authors to whom correspondence should be addressed.
b)Electronic mail: feitianshenhu@yahoo.com.
c)Electronic mail: ykim97@korea.ac.kr.

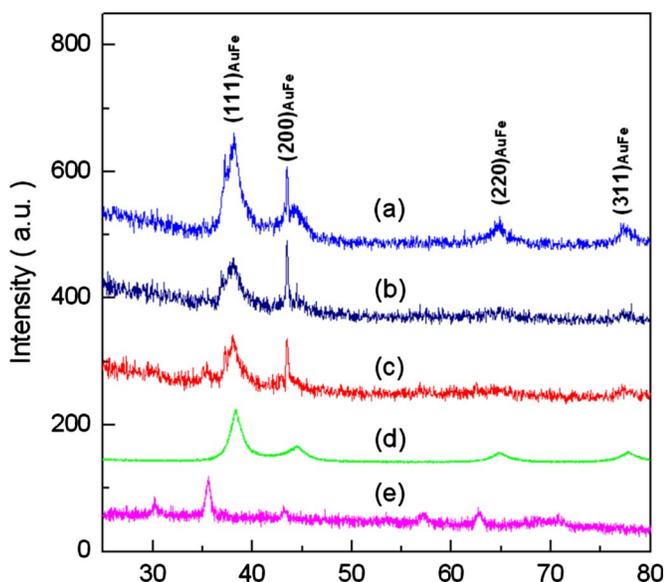FIG. 1. (Color online) XRD patterns of the AuFe nanoparticles with three compositions of (a) $Au_{0.75}Fe_{0.25}$, (b) $Au_{0.5}Fe_{0.5}$, and (c) $Au_{0.25}Fe_{0.75}$, respectively, in addition to (d) Au and (e) Fe_3O_4 obtained from the same way. The curves are shifted for clarity.

44.36°, 64.58°, and 77.44° are assigned to the AuFe positions of (111), (200), (220), and (311), which are located in the positions of the corresponding constituent materials.[15] As a result, the AuFe NPs share the same crystallographic features as that of Au and Fe, most probably a disordered face-centered cubic phase. The strong peaks, particularly positioned at 37.22° and 43.5°, point to possible formation of a stoichiometric and/or ordered cubic phase with a parameter of 4.157 Å, which is larger than the value nominally estimated from the lattices of Fe and Au. As shown in Fig. 1(e), only Fe_3O_4[16] rather than Fe was obtained in the same way starting from $Fe(acac)_3$ alone, though Au NPs were acquired with $Au(OOCCH_3)_3$ [Fig. 1(d)]. The formation of the AuFe NPs was further substantiated by the fact that all the nanoparticles as prepared could be collected by a magnetic bar, leaving no free Au particles observable and, thus, no coprecipitation of Fe and Au NPs. Furthermore, the average crystalline domain sizes of the NPs can be estimated, ∼4.7 nm for $Au_{0.75}Fe_{0.25}$, ∼4.7 nm for $Au_{0.5}Fe_{0.5}$, and ∼4.9 nm for $Au_{0.25}Fe_{0.75}$, from the full width at half maximum in terms of the Scherrer equation, if the broadening of the peaks in the XRD patterns is primarily attributed to the finite size of the nanocrystals.[17]

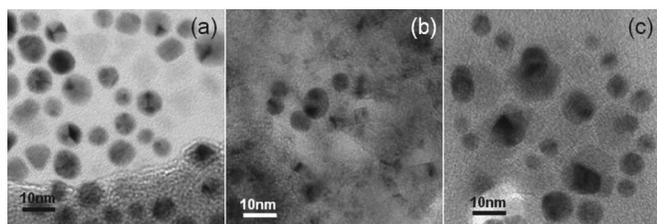The sizes and microstructures of the AuFe NPs were analyzed by TEM. Figure 2 shows the TEM morphology of

FIG. 2. TEM morphology of the AuFe nanoparticles with three compositions of (a) $Au_{0.75}Fe_{0.25}$, (b) $Au_{0.5}Fe_{0.5}$, and (c) $Au_{0.25}Fe_{0.75}$, respectively.
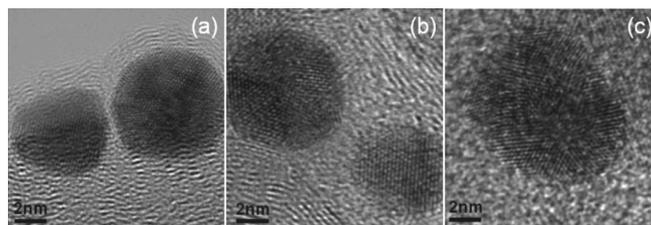

FIG. 3. High resolution TEM (HRTEM) morphology of the AuFe nanoparticles with three compositions of (a) $Au_{0.75}Fe_{0.25}$, (b) $Au_{0.5}Fe_{0.5}$, and (c) $Au_{0.25}Fe_{0.75}$, respectively.

the AuFe NPs of the three different compositions, giving particle sizes comparable to the estimation in the above. Regardless of composition, all nanoparticles are spherical in shape with a tight size distribution of ∼15% standard deviation. Examination of homogeneity in the contrast of the NPs in the images indicates that single NPs comprise several distinct sectors, which reflect the existence of twin structures in such nanoparticles as they turn out in such entities.[9,10] The observation is corroborated in the corresponding high resolution images, as shown in Fig. 3. It is evident that the nanoparticles were found to possess high crystallinity and distinct lattices for all the compositions investigated. The $Au_{0.75}Fe_{0.25}$ NPs in Fig. 3(a), which have a dominant composition of Au, show a crystallographic feature similar to their pure Au counterparts. With an iron dominant composition, the $Au_{0.25}Fe_{0.75}$ NP visualized in Fig. 3(c) consists of more, smaller crystal nanodomains, suggestive of a more random arrangement of the atoms involved despite the fact that the lattice matching between Au and Fe, as discussed previously, can be small. Given in Fig. 3(b), the nanoparticles of the $Au_{0.5}Fe_{0.5}$ composition manifest distinctive lattices, apparently with a higher degree of order than that of $Au_{0.25}Fe_{0.75}$ but less in $Au_{0.75}Fe_{0.25}$. The microstructural details of the nanoparticles observed and analyzed as a function of composition should correspondingly exert influence on their magnetic properties, as addressed below.

The magnetic properties of the AuFe NPs of various compositions were studied by a vibrating sample magnetometer at room temperature, as presented in Fig. 4. Dependent
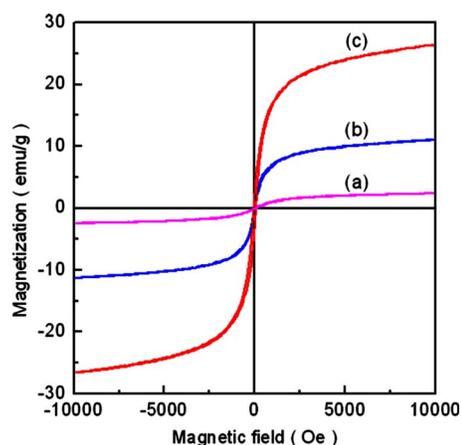

FIG. 4. (Color online) *M-H* hysteresis loops of the AuFe nanoparticles with three compositions of (a) $Au_{0.75}Fe_{0.25}$, (b) $Au_{0.5}Fe_{0.5}$, and (c) $Au_{0.25}Fe_{0.75}$, respectively.
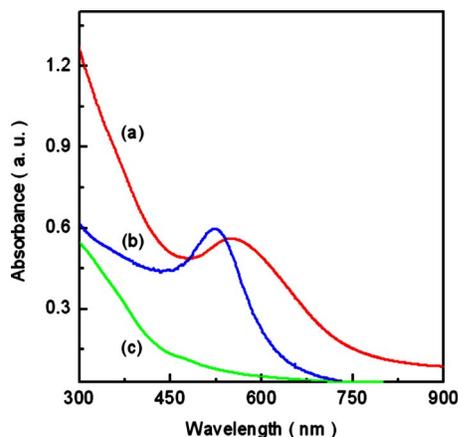
FIG. 5. (Color online) UV-visible absorption spectrum of the $Au_{0.5}Fe_{0.5}$ nanoparticles in hexane (a), compared to that of (b) Au and (c) Fe_3O_4 obtained from the same way.

on their composition, the nanoparticles show either superparamagnetic or soft ferromagnetic behavior and, as expected, an increase of magnetization with increasing Fe contents. In the case of $Au_{0.75}Fe_{0.25}$, the nanoparticles behave superparamagnetically and have a magnetization of 2.5 emu/g at 1 T, but the $Au_{0.5}Fe_{0.5}$ and $Au_{0.25}Fe_{0.75}$ NPs manifest soft ferromagnetic properties to have coercivities of 40 and 50 Oe, with magnetizations of 11.2 and 26.6 emu/g, respectively.[10,12] In fact, the magnetic property of the AuFe NPs as a function of composition is an interesting but a complex issue that needs to be handled meticulously. The phenomena may be partially interpreted in the microstructural change with the composition, which could encourage the spin-glass behavior in Au–Fe systems, in view of the experimental fact that the nanoparticles have a similar size. The M-T curves in the modes of field cooling and zero-field cooling from the SQUID measurements substantiate the typical thermal response of magnetic nanoparticles.

It is well established that nanostructured Au displays an absorption band in the visible region owing to its surface plasmon (SP), which is a characteristic of the dimension, shape, and physicochemical environment surrounding the Au nanostructure. Figure 5 shows the UV-visible spectrum of the representative $Au_{0.5}Fe_{0.5}$ NPs dispersed in hexane, compared to that of the Au and Fe_3O_4 NPs prepared in the same way. The SP resonance absorption maximum at the wavelength of about 560 nm illustrates the optical property of the gold nanostructure for the AuFe NPs, in contrast to $\sim$525 nm for the Au NPs, which have smaller dimension and no characteristic absorption for the Fe_3O_4 NPs in the range. The observation leans another support to the formation of the AuFe NPs.

Owing to the presence of Au, the AuFe NPs synthesized in the present work are readily linked to other molecules containing mercapto functional groups (e.g., 2-mercaptoacetic acid) and then are dispersible well in an aqueous solution for various purposes that request to be conducted in such a medium. The nanoparticles can be collected by an external magnetic field and well redispersed by shaking or sonication after the removal of the field. The nanoparticles prepared by the current method show a long-term stability.

IV. CONCLUSIONS

We have synthesized multifunctional AuFe alloy nanoparticles of different compositions via a polyol process and their characterization proves the integration of the optical functionality of Au and the magnetic properties of iron. The structural analysis verifies the formation of the alloy nanostructures of $\sim$5 nm in diameter with a narrow distribution of particle sizes and microstructural change with the composition. The magnetic measurement shows the composition dependence of the magnetic properties of the nanoparticles, from superparamagnetic for $Au_{0.25}Fe_{0.75}$ to soft ferromagnetic for both $Au_{0.5}Fe_{0.5}$ and $Au_{0.75}Fe_{0.25}$. Surface plasmon is observed at the absorption bands around $\sim$560 nm and the AuFe nanoparticles are rendered water soluble after thiolation.

[1]Q. A. Pankhurst, J. Connolly, S. K. Jones, and J. Dobson, J. Phys. D **36**, R167 (2003).
[2]S. Sun, C. B. Murray, D. Weller, L. Folks, and A. Moser, Science **287**, 1989 (2000).
[3]P. Tartaj, M. Morales, S. Veintemillas-Verdaguer, T. Gonzalez-Carreno, and C. J. Serna, J. Phys. D **36**, R182 (2003).
[4]M. C. Daniel and D. Astruc, Chem. Rev. (Washington, D.C.) **104**, 293 (2004).
[5]P. Mulvaney, L. M. Liz-Marzan, M. Giersig, and T. Ung, J. Mater. Chem. **10**, 1259 (2000).
[6]B. D. Busbee S. O. Obare, and C. J. Murphy, Adv. Mater. (Weinheim, Ger.) **15**, 414 (2003).
[7]Z. H. Ban, Y. A. Barnakov, V. O. Golub, and C. J. O'Connor, J. Mater. Chem. **15**, 4660 (2005).
[8]M. Chen, S. Yamamuro, D. Farrell, and S. A. Majetich, J. Appl. Phys. **93**, 7551 (2003).
[9]D. K. Saha, K. Kogab, and H. Takeo, Eur. Phys. J. D **9**, 539 (1999).
[10]K. Sato, B. Bian, and Y. Hirotsu, Jpn. J. Appl. Phys., Part 2 **41**, L1 (2002).
[11]M. Mandal, S. Kundu, S. K. Ghosh, S. Panigrahi, T. K. Sau, S. M. Yusuf, and T. Pal, J. Colloid Interface Sci. **286**, 187 (2005).
[12]I.-C. Chiang and D.-H. Chen, Adv. Funct. Mater. **17**, 1311 (2007).
[13]H. L. Liu, S. P. Ko, J. H. Wu, M.-H. Jung, J. H. Min, J. H. Lee, B. H. An, and Y. K. Kim, J. Magn. Magn. Mater. **310**, e815 (2007).
[14]B. H. An, J. H. Wu, H. L. Liu, S. P. Ko, J.-S. Ju, and Y. K. Kim, Colloids Surf., A **250**, 313 (2008).
[15]JCPDS Card No. 87-0721; JCPDS Card No. 04-0784.
[16]JCPDS Card No. 88-0315.
[17]B. D. Cullity and S. R. Stock, *Elements of X-ray Diffraction*, (Prentice-Hall, Englewood Cliffs, NJ, 2001), pp. 167–171.